

raphy on silica gel (10:1 hexane-EtOAc) gave 72 mg (30%) of pure ene adduct. The isotope effect was determined by integration of the NMR signals at 4.87 (br, 2, H transfer), 4.23 (q, 4,  $J = 6.6$  Hz, H and D transfer), 1.80 (s, 3, D transfer), and 1.37 (s, 3, H and D transfer). An identical result was obtained by integration of the  $^2\text{H}$  NMR signals at

4.87 (s, 2 D, D transfer), 1.80 (s, 3 D, H transfer), and 1.37 (s, 3 D, H and D transfer).

**Acknowledgment.** We are grateful to the National Institutes of Health for generous financial support.

## Arsenite-Inhibited Xanthine Oxidase—Determination of the Mo-S-As Geometry by EXAFS

S. P. Cramer\*<sup>1a</sup> and R. Hille<sup>1b</sup>

Contribution from the Corporate Research-Science Laboratories, Exxon Research and Engineering Company, Annandale, New Jersey 08801, and the Department of Biological Chemistry, University of Michigan, Ann Arbor, Michigan 48109. Received December 10, 1984

**Abstract:** The interaction of arsenite with oxidized, partially reduced, and fully reduced forms of xanthine oxidase has been studied by X-ray absorption spectroscopy at the arsenic and molybdenum K edges. Clear evidence for a Mo-As interaction at 3.00 Å is observed in the molybdenum EXAFS of the fully reduced ternary complex consisting of xanthine oxidase, arsenite, and the inhibitor 8-bromoxanthine. An essentially identical Mo-As distance of 3.02 Å was found for the Mo(V) complex. The accuracy of distances reported is expected to be  $\pm 0.03$  Å for first coordination sphere bonds and  $\pm 0.05$  Å for longer interactions. Surprisingly, no distinct features attributable to a Mo-As interaction are observed in the EXAFS of the oxidized enzyme, from either the molybdenum or the arsenic point of view. Furthermore, no Mo-Br interaction was observed when 8-bromoxanthine was present. For oxidized xanthine oxidase, terminal Mo=O and Mo=S bonds were observed at distances of 1.63 and 2.15 Å in the arsenite complex and 1.67 and 2.15 Å in the oxidized control sample. An additional set of thiolate-like ligands was found at 2.43 and 2.44 Å in the arsenite-inhibited and control samples, respectively. For the oxidized arsenite complex, the arsenic EXAFS suggested binding by three oxygen ligands with an average As-O distance of 1.78 Å. In the fully-reduced arsenite plus 8-bromoxanthine complex, a short Mo=O bond with a length of 1.69 Å was observed, comparable to the Mo=O distance of 1.67 Å in the uncomplexed reduced enzyme. In both cases, terminal Mo=S interactions were no longer evident. A strong Mo-S interaction, best fit by three sulfurs, was observed at average distances of 2.38 and 2.39 Å in the reduced and reduced-ternary complex data, respectively. For the latter complex, an As-S distance of 2.27 Å was calculated from the arsenic EXAFS, corresponding to at least one and more likely two As-S interactions. A weak As-O interaction at 1.78 Å was also observed. Assuming Mo-S-As bonding, and  $\pm 0.05$  Å accuracy for the distances revealed by EXAFS, a Mo-S-As angle of  $80 \pm 4^\circ$  can be derived.

### Introduction

Arsenite is a potent inhibitor of the enzyme xanthine oxidase,<sup>2</sup> and recent progress in interpretation of the EPR spectra of the Mo(V)-arsenite complex has stimulated interest in the nature of the Mo-As interaction.<sup>3-5</sup> The EPR spectra of the arsenite complex are affected by the presence of substrates and inhibitors.<sup>5</sup> It has also been shown that 8-bromoxanthine, possessing a heavy atom at the position otherwise hydroxylated by enzyme, binds to the molybdenum center of xanthine oxidase<sup>6</sup> and perturbs the Mo EPR signal of arsenite-complexed enzyme (R. Hille, unpublished). However, although the EPR spectra are rich in information about the nature of the ligands present in the Mo(V) complex, they do not yield bond lengths or angles, nor can they address the Mo(IV) and Mo(VI) oxidation states. The ternary complex consisting of arsenite-inhibited xanthine oxidase plus 8-bromoxanthine contains Mo, As, and Br centers in reasonable proximity and therefore appeared to be an ideal candidate for investigation by X-ray absorption spectroscopy.<sup>7</sup> This technique has already been used to probe the molybdenum site in uninhibited milk xanthine oxidase and liver xanthine dehydrogenase,<sup>8-10</sup> as well as other enzymes

containing molybdenum<sup>11</sup> or other metals.<sup>12</sup> In this paper, structural results are presented concerning the environment of xanthine oxidase molybdenum in the presence of arsenite under oxidized, partially reduced, and fully reduced conditions. The arsenic environment under oxidized or fully reduced conditions has also been probed.

### Experimental Section

**Sample Preparation and Handling.** Xanthine oxidase was prepared by a modification of a previously described procedure and assayed as described therein.<sup>13</sup> Enzyme thus obtained was generally in the range of 60-70% active and contained corresponding amounts of the inactive desulfo form of the enzyme. The active enzyme was separated from the inactive with use of the folate affinity column procedure of Nishino et al.<sup>14</sup> and for the present studies was enriched to greater than 92% active enzyme. Active enzyme thus prepared was concentrated to approximately 150 mg/mL with use of an Amicon PM-10 membrane. In all cases the buffer used was 0.1 M aqueous Bicine, pH 8.5. Exact concentration was determined by the absorbance at 450 nm of a 1:100 dilution of this material, which was again assayed to determine that activity had not been lost. Appropriate amounts of arsenite and/or 8-bromoxanthine were then added to known volumes of the enzyme solution and allowed to incubate for 0.5 to 1 h. Samples to be examined in the oxidized state were then transferred to lucite cells, frozen slowly with dry ice, and stored in liquid nitrogen. Those samples to be reduced were placed in the sample cells after Amicon concentration under nitrogen, treated with a twofold excess of solid sodium dithionite, capped with serum stoppers, and incubated for 1 h. At the end of the incubation

(1) (a) Exxon Research and Engineering Co. (b) University of Michigan.  
(2) Peters, J. M.; Sanadi, D. R. *Arch. Biochem. Biophys.* **1961**, *93*, 312-313.

(3) George, G. N.; Bray, R. C. *Biochemistry* **1983**, *22*, 1013-1021.

(4) Barber, M. J.; Siegel, L. M. *Biochemistry* **1983**, *22*, 618-624.

(5) Hille, R.; Stewart, R. C.; Fee, J. A.; Massey, V. *J. Biol. Chem.* **1983**, *258*, 4849-4856.

(6) Hille, R.; Stewart, R. C. *J. Biol. Chem.* **1984**, *259*, 1570-1576.

(7) Konigsberger, D., Prins, R., Eds. "Extended X-Ray Absorption Fine Structure;" John Wiley and Sons: New York, in press.

(8) Tullius, T. D.; Kurtz, D. M., Jr.; Conradson, S. D.; Hodgson, K. O. *J. Am. Chem. Soc.* **1979**, *101*, 2776-2779.

(9) Bordas, J.; Bray, R. C.; Garner, C. D.; Gutteridge, S.; Hasnain, S. S. *Biochem. J.* **1980**, *191*, 499-508.

(10) Cramer, S. P.; Rajagopalan, K. V.; Wahl, R. *J. Am. Chem. Soc.* **1981**, *103*, 7721-7727.

(11) Cramer, S. P. "Advances in Inorganic and Bioinorganic Mechanisms"; Sykes, A. G., Ed.; Academic Press: London, 1983; pp 259-316.

(12) Cramer, S. P. "Extended X-Ray Absorption Fine Structure;" Konigsberger, D., Prins, R., Eds.; John Wiley and Sons: New York, in press.

(13) Massey, V.; Brumby, P. E.; Komai, H.; Palmer, G. *J. Biol. Chem.* **1969**, *244*, 1682-1691.

(14) Nishino, T.; Nishino, T.; Tsushima, K. *FEBS Lett.* **1981**, *131*, 369-372.

a small aliquot was withdrawn and diluted into an anaerobic cuvette to ensure that excess dithionite was in fact present. The reduced samples were then frozen as described above.

At the end of the X-ray absorption measurements, the enzyme was diluted and its UV-vis spectrum recorded and assayed to monitor sample integrity. In all cases the spectra before and after X-ray exposure were the same, and no more than 10% of the activity was found to have been lost. Since the samples containing arsenite were inhibited and could not be assayed to ensure their integrity, the UV-vis absorption spectra obtained before and after acquiring the X-ray data were compared, especially in the 350–400 nm region. For the arsenic X-ray absorption samples, care was taken that the arsenite added was substoichiometric to enzyme, so that all arsenite in the sample was enzyme bound. This was verified after the X-ray experiments by assaying, which confirmed the presence of a 4% excess of uncomplexed functional enzyme.

Sodium arsenite from Baker and Adamson and  $(\text{CN}_3\text{H}_6)_2[(\text{CH}_3)_2\text{AsMo}_4\text{O}_{15}\text{H}]\cdot\text{H}_2\text{O}$ , where  $\text{CN}_3\text{H}_6 = \text{guanidinium ion}$ , were prepared as frozen solutions in pyrophosphate buffer at pH 8.5 at a concentration of 5–10 mM. The latter compound was synthesized by a literature procedure.<sup>15</sup>  $(\text{C}_5\text{NH}_6)_3[\text{Mo}_2(\text{HASO}_4)_2\text{Cl}]$ , where  $\text{C}_5\text{NH}_6 = \text{pyridinium ion}$ , was also prepared by a literature method.<sup>16</sup> 8-Bromoxanthine was synthesized as described by Fischer and Reese<sup>17</sup> by refluxing xanthine with  $\text{Br}_2$  in a sealed vial for 24 h at 95 °C.

**Data Collection.** The X-ray absorption spectra were recorded at the Stanford Synchrotron Radiation Laboratory with use of Si(2,2,0) monochromators on wiggler beam lines during 3 GeV dedicated operation. A fluorescence detection apparatus was used,<sup>18</sup> with zirconium filters for the molybdenum spectra and germanium filters for the arsenic spectra. Liquid helium temperature spectra were obtained with the aid of an Oxford Instruments cryostat. Approximately twelve 30-min scans were averaged to obtain each spectrum.

**Data Analysis.** The data were processed by using previously described procedures.<sup>19–21</sup> The curve-fitting analysis of the EXAFS was based on the following expression:

$$\chi(k) \approx \sum_s (N_s/kR_s^2) A_s(k) \exp(-2\sigma_s^2 k^2) \sin [2kR_s + \alpha_s(k)] \quad (1)$$

where  $k$  is the photoelectron wave vector,  $N_s$  is the coordination number,  $R_s$  is the absorber–scatterer distance, and  $\sigma_s^2$  is the mean square deviation of  $R_s$ . In cases where the Debye–Waller factor could not be calculated from the vibrational spectrum of the model compounds, a value for  $\sigma^2$  was estimated by fitting the spectra with a theoretical amplitude function and a scale factor.<sup>22,23</sup> Although the  $\sigma^2$  values thus obtained were chemically reasonable, the reported values could be adjusted in the future if better theoretical methods are developed. However, the calculated difference in  $\sigma^2$  between the enzyme and the model compound would not change.

Parameterized empirical phase shifts,  $\alpha_s(k)$ , and amplitude functions,  $A_s(k)$ , were used in all curve-fitting analyses. The phase shift and amplitude functions,  $\alpha(k)$  and  $A(k)$ , for Mo–O and Mo–S interactions have been described previously.<sup>20,21</sup> The additional Mo–As and As–X functions are included as supplementary material. An  $E_0$  of 11875 eV was used for all of the arsenic EXAFS, and the calibration used 11868 eV for the elemental As first inflection point. Curve-fitting analysis with these functions used two variables per component, the distance  $R$  and either the coordination number  $N$  or the disorder term  $\sigma^2$ . When a fixed  $\sigma^2$  was used, reasonable values were derived from previous work with model compounds.<sup>10,19</sup>

## Results

**Edges.** The molybdenum absorption edges for oxidized and reduced xanthine oxidase, both with and without arsenite, are shown in Figure 1. The edges are quite similar to those previously

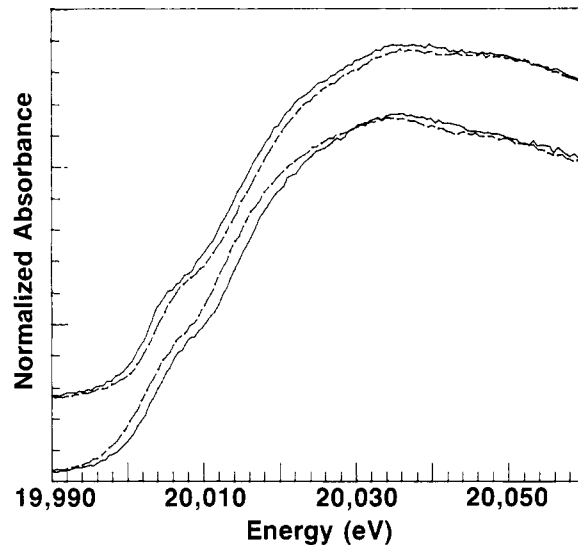


**Figure 1.** Molybdenum K absorption edge region for xanthine oxidase samples. Top: Oxidized enzyme both with (—) and without (---) arsenite. Bottom: Reduced 8-bromoxanthine complex both with (—) and without (---) arsenite. The calibration used 20003.9 eV for the molybdenum foil edge inflection point.

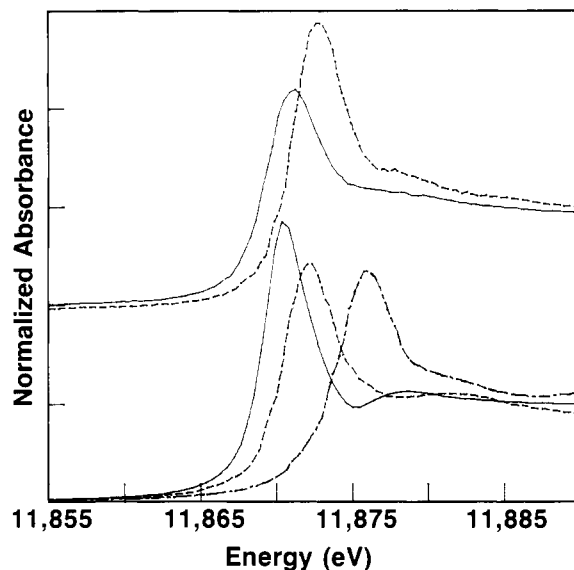


**Figure 2.** Arsenic absorption edge region for arsenite-inhibited xanthine oxidase and relevant arsenic standards. Top: Arsenite bound to oxidized xanthine oxidase (---) and As(III) bound to reduced xanthine oxidase plus 8-bromoxanthine (—). Bottom: Edges for  $\text{FeAsO}_4$  (---), As(III) in aqueous solution (···), and  $\text{As}_2\text{S}_3$  powder (—). The calibration used 11868 eV for the elemental arsenic edge inflection point.

reported for xanthine dehydrogenase,<sup>10</sup> and in all cases a low energy shoulder is observed. These shoulders are caused by strong bound state transitions which have been associated with the presence of terminal oxo or sulfido groups.<sup>24,25</sup> The control and inhibited spectra were recorded on different occasions. Therefore, it is not known whether the apparent small shifts in edge position upon arsenite binding are significant or due to slight experimental error in calibration of the monochromator.

However, significant energy shifts do occur at the arsenic absorption edge, as shown in Figure 2. Aqueous sodium arsenite and arsenite bound to oxidized xanthine oxidase have similar edges, which both occur at several eV lower energy than the As(V) edge of  $\text{FeAsO}_4$ . Furthermore, the arsenic edge shifts to even lower

(15) Barkigia, K. M.; Rajković-Blazer, L. M.; Pope, M. T.; Prince, E.; Quicksall, C. O. *Inorg. Chem.* **1980**, *19*, 2531–2537.

(16) Ribas, J.; Poilblanc, R.; Sourisseau, C.; Solans, X.; Brianso, J. L.; Miravittles, C. *Trans. Met. Chem.* **1983**, *8*, 244–250.

(17) Fischer, E.; Reese, L. *Liebigs Ann. Chem.* **1983**, *221*, 336–344.

(18) Cramer, S. P.; Scott, R. A. *Rev. Sci. Instrum.* **1981**, *52*, 395–399.

(19) Cramer, S. P.; Hodgson, K. O.; Stiefel, E. I.; Newton, W. E. *J. Am. Chem. Soc.* **1978**, *100*, 2478–2761.

(20) Cramer, S. P. "EXAFS for Inorganic Systems;" Garner, C. D., Hasnain, S. S., Eds.; Daresbury Laboratory: Daresbury, England WA4 4AD, 1981.

(21) Cramer, S. P.; Solomonson, L. S.; Adams, M. W. W.; Mortenson, L. E. *J. Am. Chem. Soc.* **1984**, *106*, 1467–1471.

(22) Teo, B.-K.; Lee, P. A. *J. Am. Chem. Soc.* **1979**, *101*, 2815–2832.

(23) Teo, B.-K.; Antonino, M. R.; Averill, B. A. *J. Am. Chem. Soc.* **1983**, *105*, 1751–1762.

(24) Cramer, S. P.; Hodgson, K. O.; Gillum, W. O.; Mortenson, L. E. *J. Am. Chem. Soc.* **1978**, *100*, 3398–3407.

(25) Kutzler, F. W.; Scott, R. A.; Berg, J. M.; Hodgson, K. O.; Doniach, S.; Cramer, S. P.; Chang, C. H. *J. Am. Chem. Soc.* **1980**, *102*, 6083–6088.

**Table I.** Representative Curve-Fitting Results for Inhibited and Control Xanthine Oxidase Samples

sample	Mo=O or As—O			Mo—S or As—S			Mo—As or As—Mo			Mo—X		residual <sup>a</sup>		
	N	R, Å	$\sigma^2$ , Å <sup>2</sup>	N	R, Å	$\sigma^2$ , Å <sup>2</sup>	N	R, Å	$\sigma^2$ , Å <sup>2</sup>	N	X			
oxidized xanthine oxidase (molybdenum edge) 263 K	1	1.68	0.00016	2	2.45	0.00296						1.878		
	2	1.67	0.00149	2	2.45	0.00237						1.497		
	1	1.67	0.00149	2	2.44	0.00534				1	S	2.15	0.00068	0.599
oxidized xanthine oxidase + As(III) (molybdenum edge) 263 K	1	1.63	0.00429	2	2.43	0.00622				1	S	2.15	0.0054	0.831
oxidized xanthine oxidase + As(III) (arsenic edge) 4 K	2	1.78	-0.00089										1.197	
	4	1.78	0.00309										1.035	
	3	1.78	0.00122										0.968	
reduced xanthine oxidase + 8BrX (molybdenum edge) 263 K				3	2.40	0.00300							1.43	
	1	1.67	0.00154	3	2.39	0.00285							0.906	
reduced xanthine oxidase + As(III) + 8BrX (molybdenum edge) 263 K	1	1.66	0.00090	3	2.40	0.00289	1	3.00	0.00875				0.848	
reduced xanthine oxidase (molybdenum edge) 4 K				3	2.38	0.00219							1.525	
	1	1.67	0.00125	2	2.38	0.00032							1.080	
	1	1.67	0.00176	4	2.38	0.00359							1.03	
	1	1.67	0.00153	3	2.38	0.00209							0.961	
reduced xanthine oxidase + As(III) + 8BrX (molybdenum edge) 4 K				3	2.39	0.00184							1.374	
	1	1.69	0.00165	3	2.39	0.00175							0.884	
	1	1.69	0.00154	3	2.39	0.00191	1	3.00	0.00967				0.797	
reduced xanthine oxidase + As(III) + 8BrX (arsenic edge) 263 K	2	1.80	0.01823	1	2.28	-0.00074	1	2.95	0.00199				1.232	
	1	1.78	0.00694	2	2.27	0.00393	1	2.95	0.00336				1.280	
Mo(V) xanthine oxidase + As(III) + 8BrX (molybdenum edge) 263 K	1	1.70	0.00252	3	2.41	0.00519	1	3.02	0.00916	1	O, N	1.98	0.00123	0.760

<sup>a</sup>See text for references to curve-fitting methods and error analyses.

energy upon reduction of the molybdenum. Since reduction below As(III) is unlikely under these conditions, this shift indicates an increase in the covalency of arsenic ligation. This would be consistent with the replacement of one or more oxygens by sulfur in the arsenic coordination sphere.

**EXAFS.** The molybdenum EXAFS Fourier transforms for oxidized and reduced active xanthine oxidase in the absence and presence of arsenite are shown in Figure 3. For the oxidized enzyme, the transform envelope for the first coordination sphere is similar in both cases, making a direct Mo—As interaction unlikely. Furthermore, although arsenite is known to bind to the oxidized enzyme with a  $K_D$  on the order of 24  $\mu\text{M}$  under the experimental conditions employed,<sup>5</sup> no unambiguous evidence for a longer distance Mo—As feature can be seen elsewhere in the transform. The Mo—As interaction might be small in the EXAFS because of a long distance, a large Debye—Waller factor, negative interference from another component, or a combination of such effects.

Arsenite binds much more tightly to reduced xanthine oxidase, with a  $K_D$  on the order of 0.2  $\mu\text{M}$ .<sup>26</sup> The EXAFS Fourier transforms for reduced forms of xanthine oxidase with and without arsenite are dominated by a pair of peaks which have previously been assigned to Mo=O and Mo—S interactions.<sup>10</sup> However, the transforms for the samples with arsenite have an additional peak at about 2.5 Å in the uncorrected transform. This new feature has a magnitude consistent with a Mo—As interaction, and a typical phase shift correction would put the true distance at 2.8–3.0 Å. In contrast, no feature assignable to a Mo—Br interaction is observed for those samples in which 8-bromoxanthine was present.

In order to be more quantitative about the structures of the native and arsenite-complexed molybdenum sites, curve-fitting analysis was used. Earlier results on oxidized xanthine dehydrogenase yielded a model with one terminal oxo group, one terminal sulfide, and a pair of thiolate-like sulfurs.<sup>10</sup> Curve-fitting the oxidized enzyme data with this model, as illustrated in Figure 4 and summarized in Table I, showed little difference between

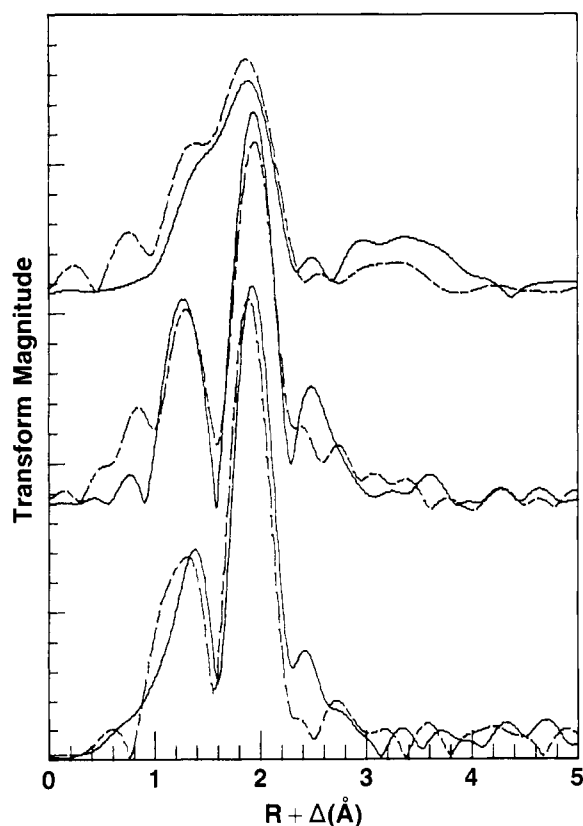


**Figure 3.** Fourier transforms for xanthine oxidase molybdenum EXAFS. Top: 263 K data for oxidized intact xanthine oxidase both with (—) and without (---) arsenite. The arsenite spectrum has had a low-frequency cutoff applied. Transform range:  $k = 4\text{--}12 \text{ \AA}^{-1}$ ,  $k^3$  weighting. Middle: 263 K data for reduced xanthine oxidase plus 8-bromoxanthine both with (—) and without (---) arsenite. Bottom: 4 K data for reduced xanthine oxidase (---) and reduced enzyme plus 8-bromoxanthine and arsenite (—). Transform range for latter four spectra:  $k = 4\text{--}14 \text{ \AA}^{-1}$ ,  $k^3$  weighting.

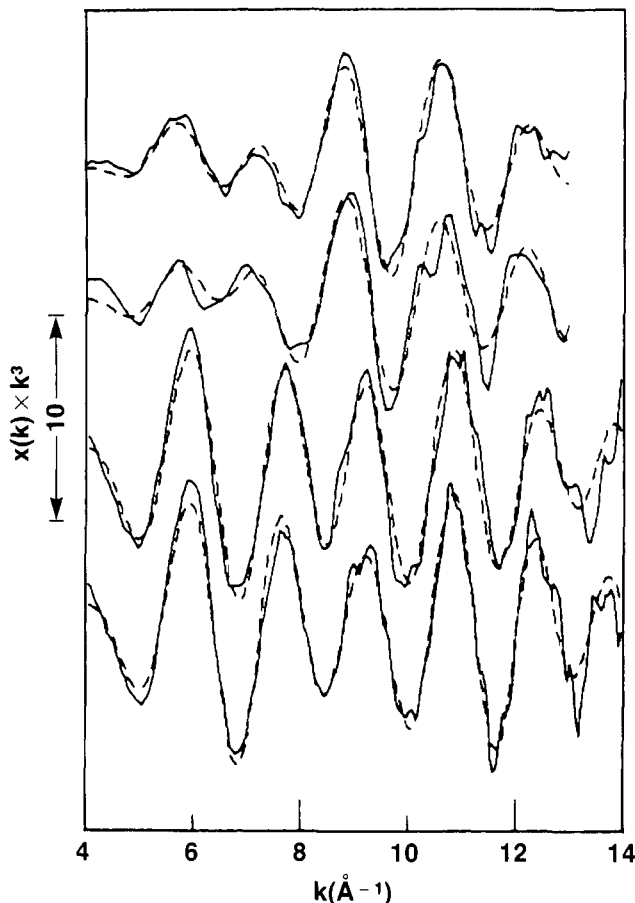


**Figure 4.** Curve-fitting analysis of molybdenum EXAFS data for xanthine oxidase. The solid line is the Gaussian-smoothed data and the dashed line is the best integer fit reported in Table I. Top to bottom: 263 K oxidized intact xanthine oxidase (XO); 263 K oxidized intact XO plus arsenite; 4 K reduced intact XO, 4 K reduced intact XO plus 8-bromoxanthine plus arsenite.

the Mo-X bond lengths for the intact forms of xanthine dehydrogenase, native xanthine oxidase, or arsenite-inhibited xanthine oxidase. The most important result is that the terminal Mo=O and Mo=S bond lengths do not change, making it unlikely that arsenite bridges across these groups in the oxidized enzyme.

Curve-fitting analysis of the reduced enzyme spectra confirmed that the terminal oxo is retained in all cases and that a substantial shortening of the thiolate-like Mo-S distance occurs. Furthermore, the short Mo=S interaction is no longer present. As shown in Table I for reduced xanthine oxidase, the number of sulfurs at 2.4 Å appears to increase to 3 upon reduction. Finally, the inclusion of a Mo-As interaction at 3.00 Å made a small improvement in the fit.

The arsenic EXAFS Fourier transforms for arsenite bound to oxidized or reduced xanthine oxidase are compared with the transforms for arsenic trisulfide and aqueous sodium arsenite in Figure 5. As with the absorption edge region, there is a strong similarity between the EXAFS of aqueous sodium arsenite and arsenite bound to oxidized xanthine oxidase. In the enzyme spectrum there is a strong As-O peak, most likely corresponding to 3 As-O bonds. Although there is a small peak at  $R + \Delta = 2.6$  Å, it is close to the noise level, and no unambiguous As-Mo interaction can be assigned. The arsenite solution spectrum has a feature at  $R + \Delta = 2.9$  Å, representing a true distance of about 3.2 Å. This feature is presumably due to some dimerization and As-O-As bonding. In this regard, although Raman spectroscopy has suggested that aqueous As(III) is primarily monomeric at high  $[\text{OH}^-]/[\text{As(III)}]$  ratios,<sup>27</sup> dimerization in the current pH and

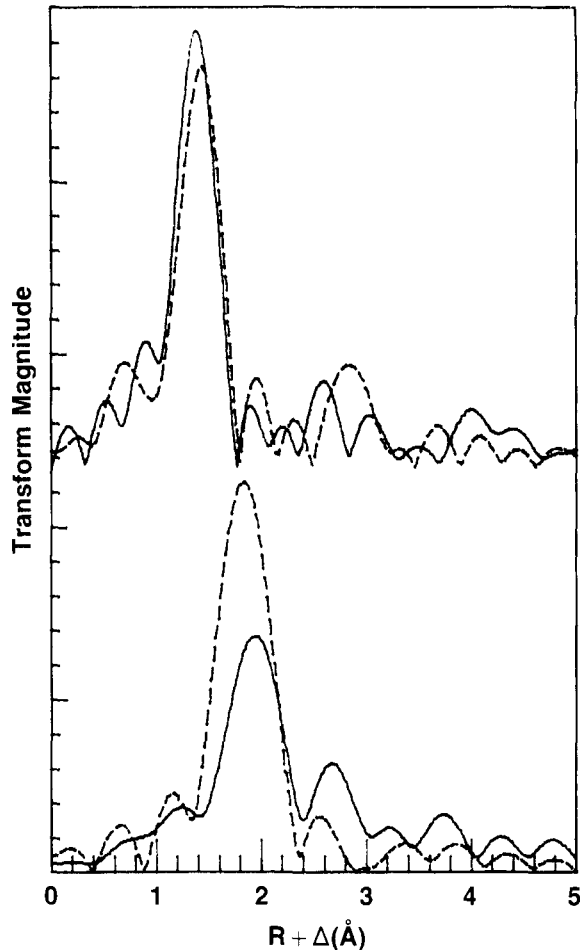


**Figure 5.** Fourier transforms of arsenic EXAFS for arsenite bound to xanthine oxidase and relevant standards. Top: 4 K data for arsenite bound to oxidize xanthine oxidase (—) and 298 K data for free arsenite in solution (---). Transform range:  $k = 4-13 \text{ \AA}^{-1}$ ,  $k^3$  weighting. Bottom: 263 K data for arsenite bound to reduced plus 8-bromoxanthine xanthine oxidase (—) and  $\text{As}_2\text{S}_3$  (---). Transform range:  $k = 4-11 \text{ \AA}^{-1}$ ,  $k^3$  weighting.

concentration regime was not ruled out.

In the reduced enzyme spectrum, the As-O feature is markedly diminished, and a new peak attributable to As-S bonding appears. The intensity is between that expected for one or two sulfurs, based on  $\text{As}_2\text{S}_3$ . Furthermore, a feature consistent with an As-Mo interaction is visible at  $R + \Delta = 2.7$  Å, corresponding to a true distance of about 3.0 Å.

In order to confirm and quantitate these assignments, curve-fitting analysis of the arsenic EXAFS was done, as illustrated in Figure 6 and summarized in Table I. For the oxidized enzyme, the spectrum could be reproduced by assuming three oxygen ligands and a single As-O distance of 1.78 Å, close to the 1.79–1.80 Å values reported for  $\text{As}_2\text{O}_3$ .<sup>28,29</sup> In contrast, the complex spectrum for reduced, arsenite-inhibited enzyme required several components for a satisfactory fit. An As-S distance of 2.27 Å was found, which is close to the 2.24 Å As-S distance in  $\text{AsS}^{30}$  and the 2.28 Å average As-S bond length found in  $\text{As}_2\text{S}_3$ .<sup>30</sup> At 1.78 Å, an As-O interaction with a large  $\sigma^2$  improved the fit. Finally, a 2.95 Å As-Mo distance was determined from the arsenic EXAFS, within experimental error of the 3.00 Å result from the molybdenum EXAFS. For various experimental reasons, the arsenic edge EXAFS spectra are of lower quality than the molybdenum data, hence the longer value is considered more accurate.

Since the primary means by which the xanthine oxidase arsenite complex has been studied has been EPR spectroscopy, a sample

(27) Loehr, T. M.; Plane, R. A. *Inorg. Chem.* **1968**, *7*, 1708–1714.

(28) Almin, K. E.; Westgrin, A. *Ark. Kemi Miner. Geol. B* **1942**, *15*, 1.

(29) Pertlik, F. *Monatsh. Chem.* **1975**, *106*, 755–762.

(30) Mullen, D. J. E.; Nowacki, W. *Z. Kristallogr.* **1972**, *136*, 48–65.

Scheme I. Previous Proposals for the Arsenite Complex Structure

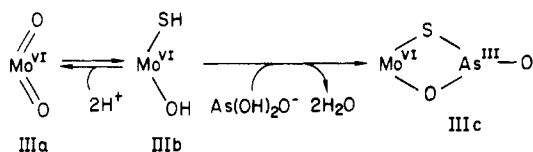
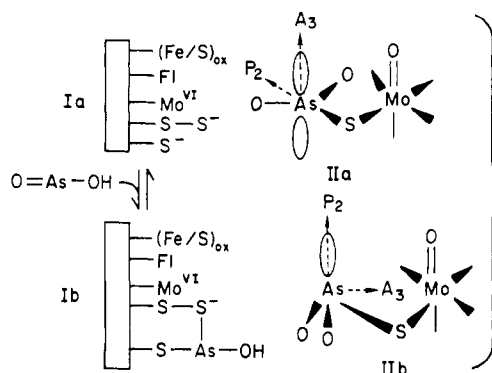


Chart I. The Local Geometry of the Arsenite-Inhibited Reduced Xanthine Oxidase Complex

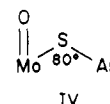
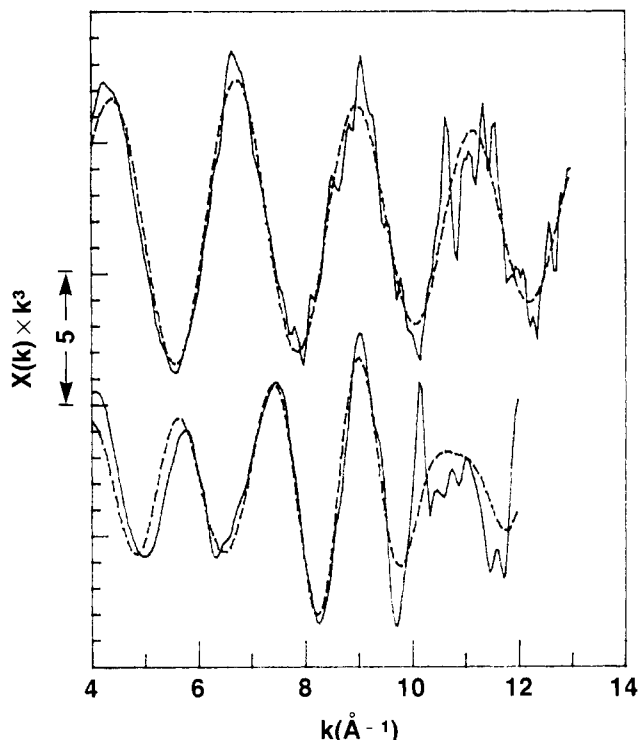
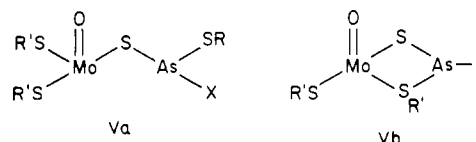


Chart II. Additional Candidates for the Partial Structure of the Arsenite-Inhibited Xanthine Oxidase Molybdenum Site



**Figure 6.** Curve-fitting analysis for arsenic EXAFS for arsenite bound to xanthine oxidase: Gaussian-smoothed data (—) and the final integer fit from Table I (---). Top: 4 K data for arsenite bound to oxidized enzyme. Bottom: 263 K data for arsenite bound to reduced enzyme plus 8-bromoxanthine.

which was predominantly Mo(V) was generated by anaerobic titration with a standardized sodium dithionite solution. Furthermore, since there was a possibility that the presence of 8-bromoxanthine changed the Mo-As distance, a reduced arsenite-inhibited sample without 8-bromoxanthine was generated. The EXAFS Fourier transforms and the curve-fitting analysis confirmed that the Mo-As distance is not dramatically changed between the Mo(IV) and Mo(V) states nor by the addition of 8-bromoxanthine, as opposed to the significant differences between the Mo(IV) and Mo(VI) structures. However, these spectra need to be recorded in better quality and at low temperatures before they can be discussed in detail.

### Discussion

A number of structures have been proposed in the literature to explain the binding of arsenite to xanthine oxidase. Massey and Edmondson suggested that arsenite reacts with a persulfide close to the molybdenum site as well as a nearby thiolate<sup>31</sup> to yield structure Ib of Scheme I. Once evidence became firm for a

terminal sulfide rather than a persulfide as the "cyanolysable sulfur" in xanthine oxidase, Bray and George interpreted their EPR data for the Mo(V)-arsenite complex in terms of structures IIa or IIb.<sup>3</sup> Finally, Hille and co-workers proposed that arsenic bridges across the terminal oxo and terminal sulfido groups of the oxidized enzyme, as in structure IIIc.<sup>5</sup>

From the current EXAFS data, it has not been possible to define the Mo-As distance for arsenite bound to the oxidized enzyme. The molybdenum EXAFS shows no significant change in the terminal Mo=O and Mo=S bond lengths, suggesting that the multiple bond character of the terminal groups is unaffected by arsenite binding. The arsenic EXAFS suggests that the arsenic first coordination sphere also remains unchanged. These combined results rule out structure IIIc and are consistent with the idea that binding of arsenite to the oxidized enzyme is an ionic interaction. Alternatively, the arsenite might bind to one or more oxygen donor ligand(s), such as protein tyrosine residues.

For the reduced enzyme, the availability of average bond lengths from both molybdenum and arsenic centers makes it possible to formulate a rather precise geometry for the Mo-S-As interaction, as illustrated in Chart I. The assumption that arsenic bridges through the terminal sulfur of active xanthine oxidase is derived from the fact that this sulfur is known to be required for strong EPR coupling.<sup>3</sup> Furthermore, the terminal oxo which would normally be cis to the terminal sulfur is placed in the expected position. The geometry shown places the As nucleus at a position for maximum magnetic interaction with the lone  $d_{xy}$  electron of the Mo<sup>V</sup>=O species<sup>31</sup> and is consistent with the strong quadrupolar interaction observed in the EPR.<sup>3</sup>

There is more ambiguity about the orientation of the remaining ligands at the Mo-S-As site, but several plausible alternatives can be considered. If there is only a single sulfur on the arsenic, then the models proposed by Bray and George are perhaps the best candidates for the arsenite complex structure. However, if the arsenic is assumed to have two sulfur ligands, then the extra sulfur could either be one already bound to molybdenum or an additional sulfur close to the active site. These alternatives are presented as additional candidates for the arsenite complex in Chart II. In this scheme the ligand X is most likely an oxygen which may or may not be protonated.

(31) Massey, V.; Edmondson, D. *J. Biol. Chem.* **1970**, *245*, 6595-6598.  
 (32) Stiefel, E. I. *Prog. Inorg. Chem.* **1977**, *22*, 1-223.

### Summary

This study has revealed dramatic differences in the binding of arsenite to oxidized and reduced forms of active xanthine oxidase. The additional As-S bond(s) observed under reduced conditions helps to explain the stronger arsenic binding to the reduced forms of the enzyme. However, the information from EXAFS raises new questions about the nature of arsenite binding. For example, it is not known what protein functional groups are involved in the binding of arsenite to the oxidized enzyme. Another important question is whether the thiolate-like sulfurs which bind molybdenum can also interact with inhibitors such as arsenite and mercury. Furthermore, there probably are additional ligands to molybdenum which still have not been identified.

Additional work is necessary to see if Mo-Br and As-Br interactions in the 8-bromoxanthine-complexed material can ever be observed. In this regard, complementary experiments using Br EXAFS are required. Since a number of substrates and inhibitors still bind to the enzyme after arsenite inhibition, it may

be possible to study the structure of such complexes from both molybdenum and arsenic points of view. Triangulation using dual or multicenter EXAFS should eventually yield geometric information unavailable from the study of a single absorption edge.

**Acknowledgment.** We thank the staff of SSRL for their assistance in making this work possible. SSRL is supported by the Department of Energy, Office of Basic Energy Science, and the National Institute of Health, Biotechnology Resource Program, Division of Research Resources.

**Registry No.** As, 7440-38-2; Mo, 7439-98-7; S, 7704-34-9; O<sub>2</sub>, 7782-44-7; arsenite, 15502-74-6; xanthine oxidase, 9002-17-9; 8-bromo-xanthine, 10357-68-3.

**Supplementary Material Available:** Parametrized Mo-X and As-X phase shift and amplitude functions used in the curve-fitting analysis (1 page). Ordering information is given on any current masthead page.

## Activation of Methane by Photoexcited Copper Atoms and the Photochemistry of Methylcopper Hydride in Solid Methane Matrices<sup>†</sup>

J. Mark Parnis, Steven A. Mitchell,<sup>‡</sup> Jaime García-Prieto, and Geoffrey A. Ozin\*

Contribution from the Department of Chemistry, University of Toronto, Toronto, Ontario, Canada M5S 1A1. Received July 8, 1985

**Abstract:** Photolysis of copper atoms at the 305–325-nm <sup>2</sup>P ← <sup>2</sup>S resonance absorption in methane matrices at 12 K results in the formation of methylcopper hydride, CH<sub>3</sub>CuH, which is characterized by a combination of IR, UV-vis, and ESR spectroscopy and <sup>1</sup>H, <sup>2</sup>H, and <sup>13</sup>C isotope-labeling experiments. CH<sub>3</sub>CuH is found to be sensitive to tail-end photolysis in a broad absorption band centered at 350 nm and extending into the 305–325-nm Cu atom region. Narrow band photolysis at 350 nm is shown to cause fragmentation of CH<sub>3</sub>CuH into CH<sub>3</sub>, H, Cu, CH<sub>3</sub>Cu, and CuH. In contrast, 10–30 K thermal annealing of matrices containing these fragments results in the reconstitution of CH<sub>3</sub>CuH. A mechanism involving a two-step reaction is proposed and supported by experimental evidence as well as by computer simulation of the growth and decay behavior of Cu, CH<sub>3</sub>, and CH<sub>3</sub>CuH as observed in ESR spectra. The types of electronic and bonding interactions which are thought to be important in the initial C-H bond insertion step are briefly discussed. The molecular structure and bonding in CH<sub>3</sub>CuH is considered in light of the experimental observations and recent theoretical proposals.

The activation of C-H bonds of saturated hydrocarbons by metal atoms and metal clusters has been the subject of extensive and diverse research in recent years.<sup>1</sup> The scope of this work encompasses reactions between alkanes and organometallic species in solution,<sup>2</sup> gas-phase atoms<sup>3</sup> and ions,<sup>4</sup> matrix-isolated atoms,<sup>5</sup> supported and unsupported heterogeneous metal and metal oxide catalysts,<sup>6</sup> and metal surfaces.<sup>7</sup> These areas may be further categorized into thermally and photolytically activated processes.

Although the experimental methodologies differ significantly between these fields, similar problems are encountered when attempting to elucidate mechanistic detail associated with the existence of short-lived, thermally and/or photolytically unstable reactive intermediates and products. Often species identification and structure determination is achieved through inference, based upon observed fragments or isotope exchange and labeling studies. The isolation and characterization of reactive intermediates re-

mains one of the major goals sought in the field of C-H bond activation.

(1) Muetterties, E. L. *Chem. Soc. Rev.* **1982**, *11*, 283–320.

(2) Parshall, G. W. *Acc. Chem. Res.* **1975**, *8*, 113. Fisher, B. J.; Eisenberg, R. *Organometallics* **1983**, *2*, 764–767. Janowicz, A. H.; Bergman, R. G. *J. Am. Chem. Soc.* **1983**, *105*, 3929–3939. Janowicz, A. H.; Periana, R. A.; Buchanan, J. M.; Kovac, C. A.; Stryker, J. M.; Wax, M. J.; Bergman, R. G. *Pure Appl. Chem.* **1984**, *56*, 13–23. Crabtree, R. H.; Mellea, M. F.; Mihelcic, J. M.; Quirk, J. M. *J. Am. Chem. Soc.* **1982**, *104*, 107–113. Hoyano, J. K.; McMaster, A. D.; Graham, W. A. G. *J. Am. Chem. Soc.* **1983**, *105*, 7190–7191. Rest, A. J.; Whitwell, I.; Graham, W. A. G.; Hoyano, J. K.; McMaster, A. D. *J. Chem. Soc., Chem. Commun.* **1984**, 624–626. Watson, P. L. *J. Am. Chem. Soc.* **1983**, *105*, 6491–6493. Jones, W. D.; Feher, F. J. *J. Am. Chem. Soc.* **1984**, *106*, 1650–1663. Bandy, J. A.; Cloke, F. G. N.; Green, M. L. H.; O'Hare, D.; Prout, K. J. *J. Chem. Soc., Chem. Commun.* **1984**, 240–242 and references cited therein.

(3) Breckenridge, W. H.; Umemoto, H. In "Dynamics of The Excited State"; Lawley, K. P., Ed.; Wiley: New York, 1982.

(4) Halle, L. F.; Houriet, R.; Kappes, M. M.; Staley, R. H.; Beauchamp, J. L. *J. Am. Chem. Soc.* **1982**, *104*, 6293–6297. Armentrout, P. B.; Halle, L. F.; Beauchamp, J. L. *J. Am. Chem. Soc.* **1981**, *103*, 6624–6628. Jacobson, D. B.; Freiser, B. S. *J. Am. Chem. Soc.* **1983**, *105*, 736–742 and references cited therein.

(5) Ozin, G. A.; Parnis, J. M.; Mitchell, S. A.; García-Prieto, J. In "Chemistry for the Future"; Grunewald, H., Ed.; Pergamon Press: New York, 1984; pp 99–105. Perutz, R. N. *Chem. Rev.* **1985**, *85*, 77–96 and references cited therein.

<sup>†</sup>In this paper the periodic group notation is in accord with recent actions by IUPAC and ACS nomenclature committees. A and B notation is eliminated because of wide confusion. Groups IA and IIA become groups 1 and 2. The d-transition elements comprise groups 3 through 12, and the p-block elements comprise groups 13 through 18. (Note that the former Roman number designation is preserved in the last digit of the new numbering: e.g., III → 3 and 13.)

<sup>‡</sup>Present address: National Research Council of Canada, Ottawa, Ontario, Canada K1A 0R5.